Valorization of waste-derived starch for the development of bioplastics for sustainable packaging applications

Materials Today Chemistry 53 (2026) 103591

Contents lists available at ScienceDirect

Materials Today Chemistry

journal homepage: www.journals.elsevier.com/materials-today-chemistry/

Valorization of waste-derived starch for the development of bioplastics for sustainable packaging applications

Shima Jafarzadeh [a,b,*], Peng Wu [c], Moon Paul [c], Zeinab Qazanfarzadeh [d], Colin J. Barrow [a,e], Omid Zabihi [c], Wendy Timms [a,b,**], Minoo Naebe [a,c,***]

[a] Centre for Sustainable Bioproducts, Deakin University, Geelong, Victoria, 3216, Australia
[b] School of Engineering, Deakin University, Geelong, Victoria, 3216, Australia
[c] Institute for Frontier Materials (IFM), Deakin University, Waurn Ponds, VIC, 3216, Australia
[d] Division of Industrial Biotechnology, Department of Life Sciences, Chalmers University of Technology, 412 96, Gothenburg, Sweden
[e] Distinguished Research Fellow, College of Health Sciences, Abu Dhabi University, Abu Dhabi, 59911, United Arab Emirates

ARTICLE INFO

Keywords:
Bread waste
Biodegradable films
Sago starch
Polyvinyl alcohol
Mechanical properties
Sustainable packaging

ABSTRACT

This study explores the development of cost-effective, bioplastic packaging films by incorporating food waste-derived starch to reduce production costs while maintaining functional performance. Starch was extracted from bread waste and blended with sago starch and polyvinyl alcohol (PVA) in various ratios to evaluate the impact of low-cost, waste-derived materials on mechanical, thermal, optical, physicochemical, and barrier properties. The objective was to identify optimal formulations that balance performance and economic feasibility. FTIR and XRD analyses confirmed hydrogen bonding and amorphous structures contributing to film flexibility. Surface analysis revealed smoother morphologies in PVA blends and increased hydrophilicity in sago starch films. The bread starch–PVA blend (PB 2:2) exhibited the best mechanical properties (15.5 MPa tensile strength, 259.99% elongation), while also achieving excellent UV-blocking (0% transmittance at 294 nm) and high transparency (90%). The incorporation of sago starch increased thermal stability compared to Control and PB films, particularly in the second and third decomposition stages, while PB (2:2) films exhibited the best moisture barrier properties (WVTR 670.84 g/m^2·24 h). The findings demonstrate the potential of bread waste as a viable raw material for bio-based packaging. The PB (2:2) formulation offered optimal performance and the lowest cost, supporting a sustainable strategy for replacing synthetic polymers with renewable, food-waste-derived starch.

1. Introduction

Environmental degradation remains one of the most critical challenges of our time, driven by a range of unsustainable human activities. Among the most urgent issues are food waste and plastic pollution, both of which have far-reaching ecological and economic impacts [1,2]. For example, Australia generates 2.5 million tons of plastic waste annually, which is expected to double by 2040 if unaddressed [3]. At the global level, plastic waste is responsible for the deaths of over 100 million marine animals annually. Moreover, as plastic waste breaks down, it releases carbon dioxide and other harmful gases into the atmosphere, contributing to global warming, climate change, and environmental issues such as acid rain [4]. Transitioning to environmentally friendly materials for food packaging offers an effective means to reduce the range of environmental problems associated with plastic pollution.

Similarly, food waste has significant economic implications on a global scale, with countries incurring substantial financial losses. For instance, in Australia alone, food waste is estimated to cost the national economy approximately $36.6 billion annually [2,5]. Therefore, a promising approach to tackle the dual challenges of plastic pollution and food waste is biomass refining, a process that transforms food waste biomass into valuable, sustainable products. This approach not only diverts organic waste from landfills but also offers a renewable alternative to fossil-based plastics, contributing to a more circular and

* Corresponding author. Centre for Sustainable Bioproducts, Deakin University, Geelong, Victoria, 3216, Australia.
** Corresponding author. Centre for Sustainable Bioproducts, Deakin University, Geelong, Victoria, 3216, Australia.
*** Corresponding author. Centre for Sustainable Bioproducts, Deakin University, Geelong, Victoria, 3216, Australia.
E-mail address: s.jafarzadeh@deakin.edu.au (S. Jafarzadeh).

https://doi.org/10.1016/j.mtchem.2026.103591
Received 3 November 2025; Received in revised form 3 April 2026; Accepted 4 April 2026
Available online 8 April 2026

environmentally responsible economy.

Bread is one of the most widely consumed staple foods globally, playing a crucial role in the diet of millions of people. However, it is also one of the most wasted food products, contributing significantly to global food loss and waste. In Australia, bread waste ranks among the top five sources of food waste, with around 20% of bread produced being discarded, equating to millions of loaves annually [6]. Beyond the economic impact, discarded bread generates methane emissions when decomposed in landfills, exacerbating environmental pollution [7]. Bread, a complex of gluten-starch, can be utilized to produce starch-based materials [8]. This effect is more pronounced when the extraction method involves minimal processing and uses water as the only solvent. Starch-based films have emerged as promising substitutes for conventional petroleum-based plastics due to their abundance, renewability, and biodegradability [9]. However, pure starch films, due to their hydrophilic nature, exhibit inherent limitations such as poor mechanical strength, high moisture sensitivity, and low water vapor barrier properties, which restrict their wide application in food packaging [10]. Blending has emerged as a promising strategy to overcome these limitations in polysaccharide-based films and coatings [11]. Therefore, starch, extracted from bread waste, can be blended with natural polymers such as sago starch and synthetic polymers like polyvinyl alcohol (PVA) to create bioplastics with improved mechanical and barrier properties [12,13]. Sago starch, recognized for its high purity and excellent gelatinization properties, has shown promise when blended with PVA and plasticizers like glycerol or sorbitol, resulting in bioplastics with enhanced tensile strength and biodegradability [14].

While studies have demonstrated the feasibility of using agricultural byproducts for bioplastics [15–21] bakery byproducts, such as stale bread, are largely underutilized. Hence, this study aims to investigate the potential of transforming bread waste into bioplastic films by incorporating either sago starch or polyvinyl alcohol (PVA). The study will focus on optimizing the formulations to enhance the mechanical strength, flexibility, and moisture resistance of the resulting bioplastics. This research contributes to both waste reduction and the advancement of sustainable packaging technologies, paving the way for commercially viable, eco-friendly alternatives to conventional materials.

2. Materials and methods

2.1. Materials

Stale household bread (originating from wheat starch, which typically contains ~25% amylose and ~75% amylopectin) was collected locally and dried at 50 °C for 24 h in a hot air oven until a constant weight was achieved. The dried bread was ground into a fine powder using a laboratory grinder and sieved through a 60-mesh sieve to obtain a uniform particle size. Sago starch, sourced from *Metroxylon sagu* (sago palm) (Amylose amylose content: 24% – 28%, Amylopectin amylopectin content: 72% – 76%, molecular weight; 20 × 106) was obtained from the local market and polyvinyl alcohol (PVA, molecular weight 85,000–124,000, 99% hydrolyzed) was purchased from Merk. Glycerol (≥99% purity) was used as a plasticizer and was obtained from Merck. All other chemicals and reagents used were of analytical grade.

2.2. Extraction of starch from bread waste

The starch from stale bread was extracted using a modified wet-extraction method [22]. The finely ground bread powder was mixed with distilled water at a 1:10 (w/v) ratio and stirred continuously for 1 h at room temperature. The resulting slurry was filtered through muslin cloth to separate the solid residues, and the filtrate was allowed to settle at 5 °C for 12 h to facilitate starch sedimentation. The supernatant was discarded, and the starch sediment was washed repeatedly with distilled water to remove salts and other impurities. The washed starch was freeze-dried for 48 h, ground, and sieved to obtain a fine starch powder. The extracted starch was stored in an airtight container at room temperature for further use in bioplastic formulation.

2.3. Preparation of bioplastic films

Bioplastic films were developed using bread-derived starch, either alone or in combination with sago starch or polyvinyl alcohol (PVA). For starch-based blends, bread starch was mixed with sago starch at weight ratios of 2:2 and 1:3, coded as SB(2:2) and SB(1:3), respectively. Similarly, bread starch was blended with PVA at the same ratios, resulting in formulations labeled PB(2:2) and PB(1:3). In addition, control films composed solely of bread starch (Control), sago starch (Sago), or PVA were prepared as reference materials. Each component, bread starch, sago starch, and PVA, was dissolved in distilled water at 90 °C under continuous stirring to ensure complete homogenization. Glycerol (40% w/w of solid content) was incorporated as a plasticizer to enhance film flexibility. The resulting solutions were cast into Petri dishes and dried at 40 °C for 24 h using a hot air oven. After drying, films were carefully peeled off and conditioned at 23 °C with 50 ± 5% relative humidity for 48 h prior to characterisation. Table 1 provides detailed compositions, including control films made from pure bread starch and individual component films (sago starch and PVA) for comparison and Figs. 1 and 2 illustrate schematic of the process for fabricating bioplastic using extracted bread waste starch blended with sago starch or PVA and photographs of the prepared bioplastic films respectively.

2.4. Characterization of composite films

2.4.1. Chemical properties and microstructure

The chemical composition and functional groups of the films were analyzed using a Bruker INVENIO FT-IR spectrometer. Spectra were recorded in the 500–4000 cm^{-1} range in absorbance mode with 64 scans and a resolution of 4 cm^{-1}. XRD analysis was conducted using an X'pert Powder XRD diffractometer with Cu-Kα radiation (λ = 1.5418 Å) to determine the crystalline structure. Scans were performed in the 2θ range of 5–115° with a step size of 0.013°. SEM imaging was performed using a ZEISS GeminiSEM 460 microscope with an accelerating voltage set to 5 kV. To improve conductivity, the samples were coated with a 5 nm gold layer using a Leica ACE600 sputter coater. Surface roughness and nanoscale topography of the bioplastic films were analyzed using Atomic Force Microscopy (AFM) to investigate their surface characteristics at the nanoscale. The AFM measurements were performed for films (air contact side) using a Bruker Dimension Icon AFM system equipped with a silicon nitride cantilever with a nominal spring constant of 0.4 N/m and a tip radius of approximately 2 nm. The AFM scans were conducted in PeakForce Tapping mode under ambient conditions (temperature of 23 ± 2 °C and relative humidity of 40–50%) to minimize environmental effects on the film surfaces. A scan area of 1 μm × 1 μm was selected to capture detailed nanoscale features, with a scan rate of 0.5 Hz and a resolution of 512 × 512 pixels. The 3D topography images were generated, and surface roughness parameters, including Root Mean Square roughness (RMS), Average roughness (Ra), and Maximum roughness height (Rmax), were calculated using the NanoScope Analysis software (version 1.9, Bruker). The data were processed by applying a second-order plane fit and flattening to remove background tilt and

Table 1
Composition of bioplastic film treatments.

Treatment Code	Bread Starch (g)	Sago Starch (g)	PVA (g)	Glycerol (g)
Bread Starch	4g	0	0	1.6g
Sago	0	4g	0	1.6g
PVA	0	0	4g	1.6g
SB(2:2)	2g	2g	0	1.6g
SB(1:3)	3g	1g	0	1.6g
PB(2:2)	2g	0	2g	1.6g
PB(1:3)	3g	0	1g	1.6g

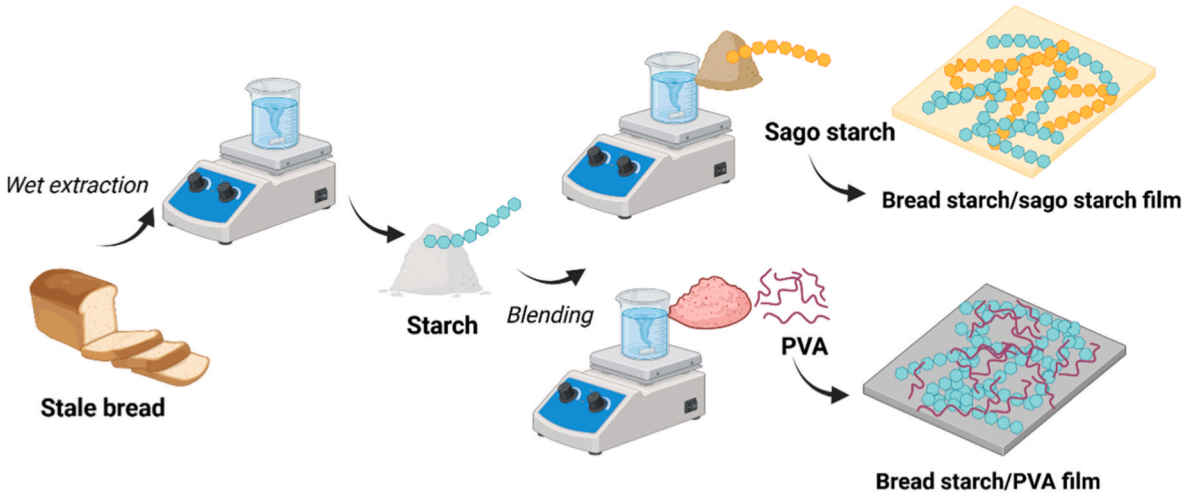

Fig. 1. Schematic illustration of the process for fabricating bioplastic using extracted bread waste starch blended with sago starch or PVA.

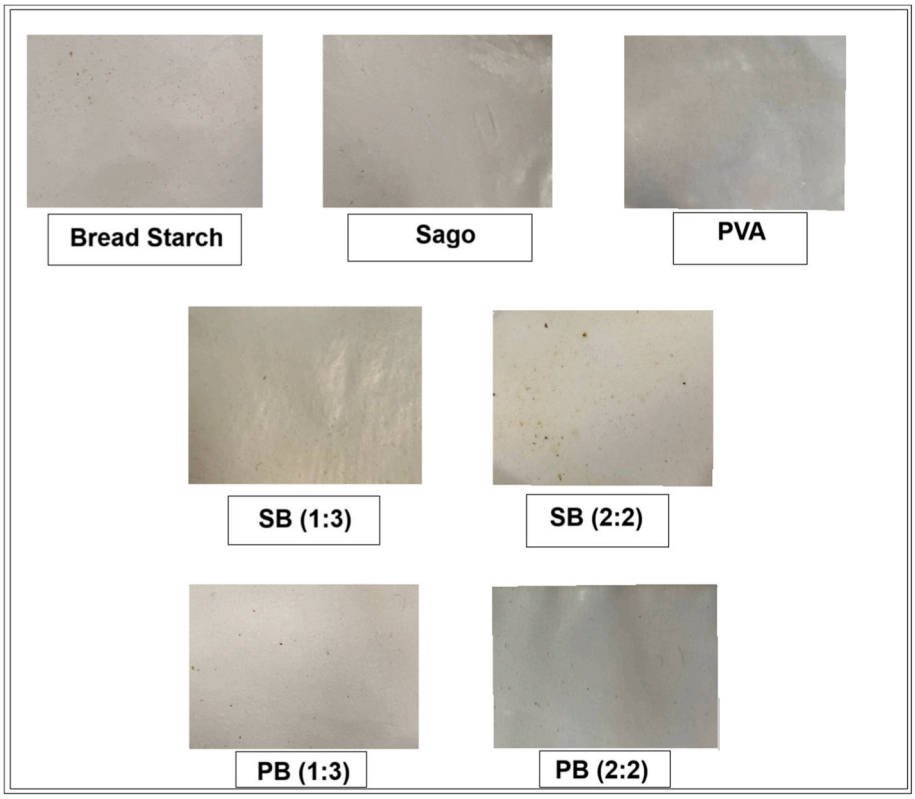

Fig. 2. Photographs of the prepared bioplastic films illustrating their visual appearance.

noise, ensuring accurate roughness measurements.

2.4.2. Optical properties

The optical properties of the composite films were examined using a Shimadzu UV-2600 UV-Vis spectrophotometer (Japan) across a wavelength range of 200–800 nm to evaluate their UV-Vis light transmittance and absorbance. The transmittance spectra were recorded to assess the transparency of the films, while the absorbance spectra provided information on their capacity to block ultraviolet (UV) light. The color indices of the films were analyzed using a Datacolor 600 spectrophotometer. The total color difference (ΔE) was calculated using the following equation:

$$\Delta E = \sqrt{(\Delta L^*)^2 + (\Delta a^*)^2 + (\Delta b^*)^2} \quad \text{Eq.(1)}$$

where ΔL*, Δa*, and Δb* are the differences between the corresponding color parameters of the samples and those of the white standard (L* = 93.56, a* = − 1.31, b* = 0.23) [11].

2.4.3. Thermal properties

The thermal properties of the composite films were evaluated using a Thermogravimetric Analyzer (TGA), model Discovery 550 Auto (TA Instruments, USA). In this analysis, film samples weighing 5–10 mg were placed in the TGA instrument, and the thermal degradation behavior was observed by heating the samples from room temperature to 600 °C

at a constant heating rate of 10 °C/min. The analysis was conducted under a nitrogen atmosphere to prevent oxidation, which could interfere with the thermal degradation process [11].

2.4.4. Water vapor permeability

The Water Vapor Transmission Rate (WVTR) was determined using the gravimetric desiccator method as described in ASTM E96/E96M-22ae1. In this method, circular film specimens were carefully sealed onto test cups containing distilled water. These cups were then placed inside a desiccator, where the relative humidity was maintained at around 0% by using anhydrous calcium chloride as a desiccant. This setup created a controlled environment where water vapor would naturally diffuse through the film and into the desiccator. The weight changes of the test cups were meticulously recorded over two different time periods: 5 days and 7 days, using a high-precision analytical balance with an accuracy of ±0.0001 g. The weight loss over time was directly related to the amount of water vapor that passed through the film. The WVTR was then calculated using the following equation:

WVTR was calculated using the equation:

$$WVTR = \frac{\Delta W}{A^{*}T} \quad \text{Eq.(2)}$$

where ΔW is the weight change (g) over time T (days), and A is the exposed film area (m^2) [11].

2.4.5. Contact angle measurement

The hydrophobicity of the composite films was evaluated using the sessile drop method with a Biolin Theta Flow Tensiometer. In this method, a 10 μL deionized water droplet was carefully placed on the surface of the film, and the contact angle was determined by analyzing the shape of the droplet. The contact angle represents the angle formed between the baseline of the droplet and the tangent line at the point of contact between the droplet and the film surface.

2.4.6. Mechanical properties

The mechanical properties of the composite films were assessed (temperature of 23 ± 2 °C and relative humidity of 40–50%) using an Instron Universal Testing Machine (Instron 3369, USA), with a 100 kN load capacity. The tests followed ASTM D882-10 standards, which specify the method for measuring the tensile properties of films. Rectangular film specimens with dimensions of 30 mm length, 15 mm width, and 0.1 mm thickness were prepared for testing. These samples were subjected to tensile testing at a constant crosshead speed of 10 mm/min. During the testing, the tensile stress, elongation at break, and Young's modulus were recorded from the resulting stress-strain curves.

2.5. Statistical analysis

All experiments were performed in triplicate, and data were expressed as mean ± standard deviation. Statistical analyses were conducted using SPSS v26.0 (IBM, USA). One-way analysis of variance (ANOVA) followed by Tukey's post-hoc test was used to determine significant differences ($p < 0.05$) between treatments.

3. Results and discussion

3.1. FTIR analysis

FTIR spectroscopy was used to analyze the molecular structure and interactions within the films formulated from bread waste starch, sago starch, PVA, and glycerol. The FTIR spectra display characteristic absorption bands corresponding to the major functional groups present in the components (Fig. 3).

A broad O–H stretching band between 3200 and 3600 cm^{-1} was observed across all film samples. This band is associated with the hydroxyl groups of starch, PVA, and glycerol, as well as bound water. It appeared broader in the pure starch-based films (Control and Sago) and more intense in PVA, consistent with extensive hydrogen bonding and a higher concentration of hydroxyl groups, respectively [23]. In contrast, the intensity of the O–H band decreased in composite films containing PVA, particularly in PB(1:3), suggesting hydrogen bonding between starch and PVA. This interaction reduces the number of free hydroxyl groups. The peaks at 2750-300 cm^{-1} in all the film spectra corresponded to C–H stretching vibrations [22].

A distinct C═O stretching band around 1650 cm^{-1} was observed only in the PVA-containing composite, verifying the incorporation of PVA into the matrix. The band was more intense in PB(2:2), likely due to the higher proportion of PVA in this formulation [23].

The C–O–C stretching vibrations, typically found between 1000 and 1200 cm^{-1}, were evident in all starch-containing films, attributed to the glycosidic linkages in starch molecules. Notably, a slight shift in peak position was detected, for example, from 1080 cm^{-1} in the Control to 1083 cm^{-1} in SB(2:2) indicating interactions between glycerol and the starch matrix. These interactions, particularly plasticization by glycerol, enhance polymer chain mobility and film flexibility [24]. The peak broadening observed in SB(1:3) and PB(1:3) suggests a greater influence of glycerol, consistent with increased plasticization at lower sago starch or PVA content [25].

In the fingerprint region (500–1000 cm^{-1}), overlapping absorption peaks were observed in the composite films, reflecting the complexity of molecular interactions among starch, PVA, and glycerol. Importantly, no new absorption bands were detected in the composite films compared to

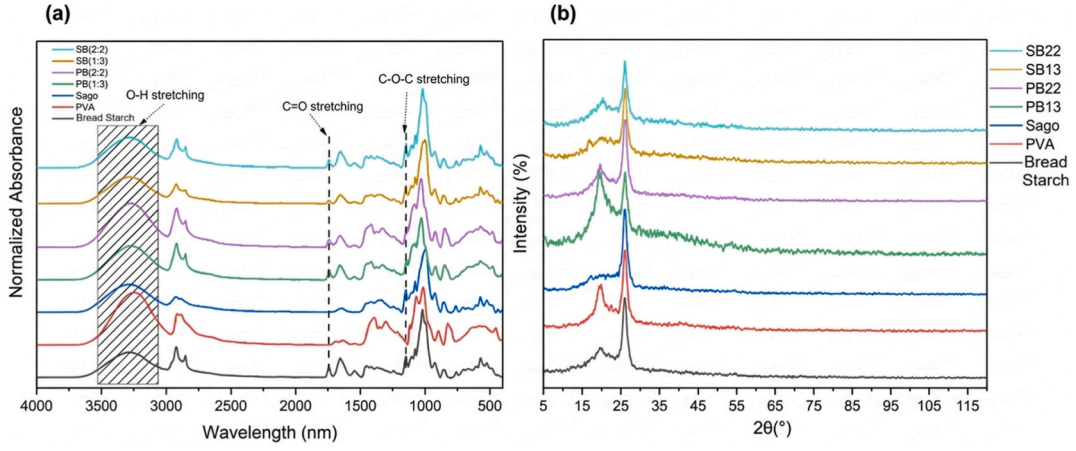

Fig. 3. (a) FTIR spectra of bread starch, sago starch, PVA films, and their blend in the wavenumber range of 500–4000 cm^{-1}, (b) and their XRD patterns in the 2θ range of 5–115°.

the individual components, confirming that the interactions are physical rather than chemical. This implies the absence of covalent bonding and the presence of non-covalent interactions such as hydrogen bonding and van der Waals forces, which are critical in forming compatible and functional polymer blends [26]. The FTIR spectra indicate the presence of intermolecular interactions among bread starch, sago starch, PVA, and glycerol, as evidenced by band shifts, peak broadening, and changes in intensity consistent with spectra reported for starch–PVA blend films [24].

3.2. X-ray diffraction (XRD) analysis

XRD analysis was conducted to assess the crystalline structure and modifications in the bioplastic films. As shown in Fig. 3, the XRD patterns revealed distinct differences among the formulations. The Control film exhibited prominent peaks at $2\theta \approx 16^\circ$, 19°, and 26°, characteristic of the A-type crystalline structure of cereal starches [9]. The Sago film displayed similar peaks with lower intensity at 19°. In contrast, the PVA film showed a broad peak at 19.5°, indicative of its semi-crystalline nature, whereas peaks appearing above 20° are likely attributable to impurities [27]. For SB(2:2) and SB(1:3), starch-related peaks at 16°, 19°, and 26° diminished in intensity, with broader, flatter patterns beyond 25°, suggesting an amorphous structure. The higher sago starch content in SB(2:2) led to a more pronounced reduction in peak intensity than in SB(1:3), likely due to glycerol's plasticizing effect, disrupting starch crystallinity [12]. For PB(2:2) and PB(1:3), starch peaks overlapped with PVA peak centered at 19.5. PB(2:2), with higher PVA content, showed a flatter profile than PB(1:3), confirming that increased PVA more effectively disrupts starch crystallinity [28]. However, in the lower quantity of PVA in the PB(3:1) film, structural reorganization of PVA domains was promoted in the highly plasticized starch matrix, leading to increased crystalline ordering as evidenced by peak sharpening at 19.5°.

3.3. Surface morphology

The surface morphology of bioplastic films was analyzed using SEM to investigate the structural characteristics that influence their performance. The corresponding micrographs are presented in Fig. 4. The control film exhibited a highly rough and heterogeneous surface characterized by visible irregularities and a porous structure. This roughness is likely due to the presence of non-starch water-soluble compounds and salts extracted along with starch from the stale bread [22]. The sago film displayed a smoother surface with few granular and fragmented appearances. This fragmented structure is likely due to the high amylopectin content of sago starch or the presence of impurities [29].

The SB films, which combine sago starch with bread starch, showed surfaces that were slightly more uniform than Control but still exhibited roughness and granular features. The surface of SB(1:3) appeared slightly rougher with more pronounced granules, while SB(2:2) displayed a marginally smoother texture, possibly due to the higher proportion of sago starch enhancing molecular interactions to a limited extent [30]. However, the overall roughness and lack of a cohesive matrix in both SB films indicate that blending sago starch with bread starch does not significantly improve film uniformity. Similar to the sago starch film, the PVA film exhibited a smooth surface with some dispersed particles due to PVA's long, flexible polymer chains, which form a continuous and cohesive film matrix [31]. The SEM image of PB (2:2) shows a surface with fewer irregularities compared to the starch-based films, however, PB (1:3) displayed an even smoother and more uniform surface with minimal visible irregularities. This observation indicates better compatibility between bread starch and PVA at lower PVA content, promoting stronger hydrogen bonding between the polymer chains and resulting in a more cohesive and compact matrix. This is further supported by the XRD results, which showed an increase in structural ordering. Boonsuk et al. [32] similarly reported that PVA in starch blends enhanced film morphology, leading to smoother surfaces [32].

3.4. Surface roughness analysis

Atomic Force Microscopy (AFM) was utilized to evaluate the surface roughness and nanoscale topography of the bioplastic films, providing insights into how surface characteristics influence their mechanical properties and suitability for food packaging applications. The AFM results, including surface roughness parameters such as Root Mean Square roughness (RMS), average roughness (Ra), and maximum roughness height (Rmax) are summarized in Table 2, while the 3D topography images are presented in Fig. 4.

The control film exhibited the highest surface roughness among all treatments, with an RMS of 257 nm, Ra of 184 nm, and Rmax of 1525 nm. Its 3D topography image reveals a highly uneven surface with prominent peaks and valleys, confirming a rough and irregular structure. The surface roughness of the control film was significantly higher than that of raw starch films previously reported at 6.238 nm, which might be due to the presence of impurities (Chai et al., 2009). This observation is consistent with the SEM results, which also showed a rough and porous surface for the Bread starch film.

The sago film had a significantly smoother surface compared to the control, with an RMS of 21.6 nm, Ra of 17.2 nm, and Rmax of 124 nm. The 3D topography image of sago shows a less uneven surface with smaller peaks, indicating a more uniform structure than the control. This observation is likely due to its purity and high amylopectin content, which enhances molecular interactions and reduces aggregation [29].

The SB films, blending sago starch with bread starch, displayed intermediate roughness values. SB(2:2) appears slightly smoother than SB (1:3), likely due to the higher proportion of sago starch, which contributes to better molecular interactions [30]. The 3D topography images of SB(1:3) and SB(2:2) reveal surfaces with moderate peaks and valleys, less rough than the control but more uneven than sago. The neat PVA film exhibited the lowest surface roughness among all formulations. Its incorporation into the blends reduced the surface roughness of bread starch films more significantly than that of sago starch films. Consistent with SEM observation, lower PVA content in PB(1:3) showed lower roughness compared to PB(2:2). This observation was also confirmed in the 3D topography image of PB blends. However, the smoother surface of PB(1:3) compared to PB(2:2) is unexpected, as higher PVA content typically leads to smoother surfaces due to better compatibility with starch [33]. Popescu et al. [34] reported that increasing starch content in PVA/starch blends increases surface roughness (RMS from 20 to 25 nm for PVA to 77-102 nm for 50% starch), but adding cellulose nanocrystals (CNC) can reduce roughness at higher concentrations due to better dispersion [34]. Similarly, Jayasekara et al. (2004) reported that pure PVA films have low surface roughness, consistent with the findings here, and blending with starch increases roughness due to phase separation, as seen in PB films. This finding also aligns with Boonsuk et al. [32], who reported that PVA enhances surface uniformity in starch blends, leading to improved mechanical properties [32].

3.5. UV-Vis spectroscopy

UV-Vis spectroscopy was conducted to evaluate the optical properties of the bioplastic films, specifically their UV-blocking ability and transparency, across the wavelength range of 200–800 nm. The transmittance spectra of the films, including bread strach, sago, PVA, PB(2:2), PB(1:3), SB(2:2), and SB(1:3) are presented in Fig. 5.

The Bread starch film demonstrated exceptional UV-blocking properties, with transmittance dropping to 0% at 294 nm in the UV region (200–400 nm). This strong UV absorption is likely due to chromophores present in bread starch, such as proteins or phenolic compounds [10]. In contrast, the Sago film exhibited higher UV transmittance, recording

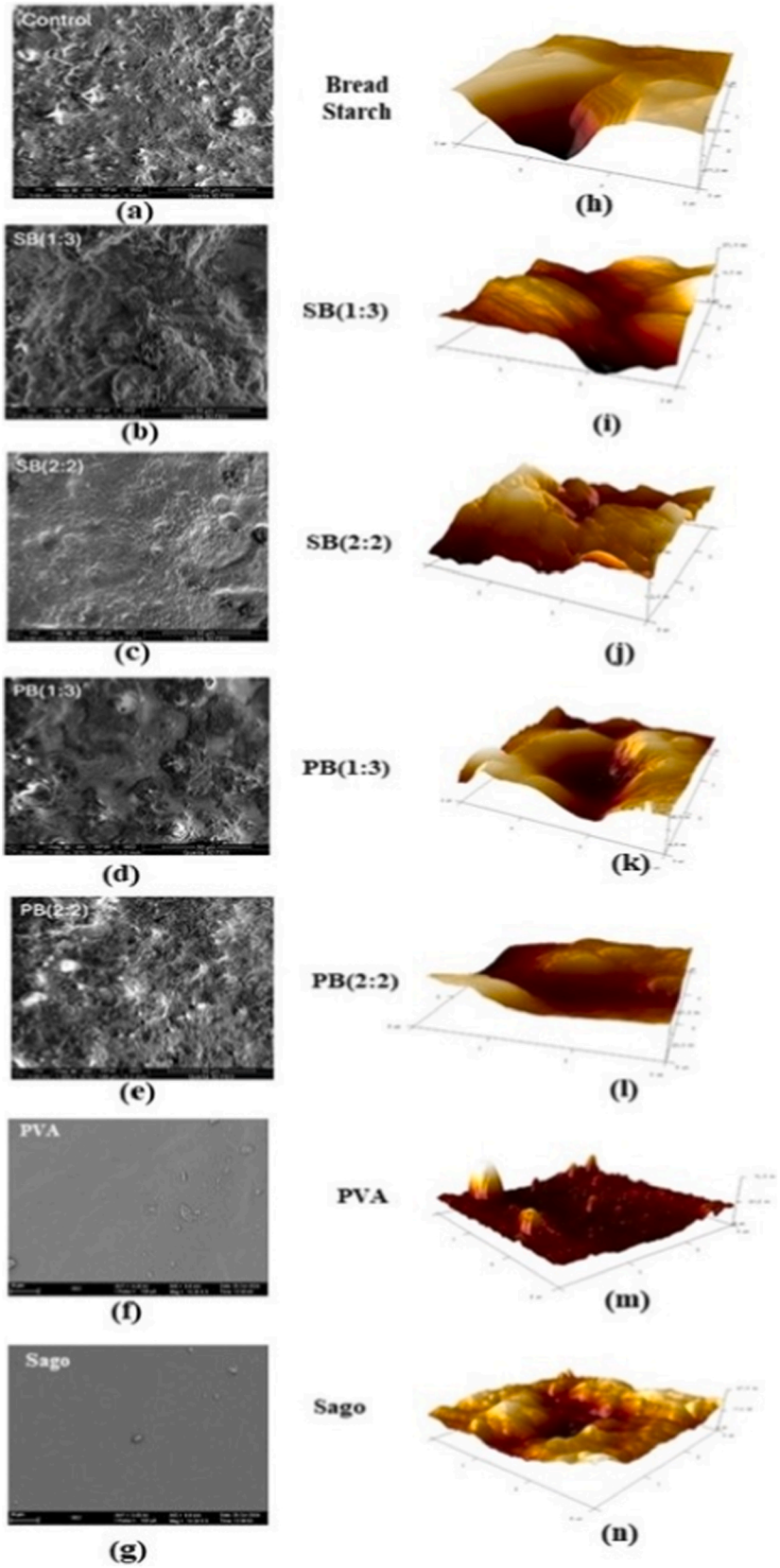

Fig. 4. Morphology and nanoscale roughness of bioplastic films. **(a–g)** SEM images of (a) Bread Starch, (b) Sago, (c) PVA, (d) SB(2:2), (e) SB(1:3), (f) PB(2:2), and (g) PB(1:3), showing surface texture. Scale bars: 10 μm. **(h–n)** AFM 3D topography images of (h) Bread Strach, (i) Sago, (j) PVA, (k) SB(2:2), (l) SB(1:3), (m) PB(2:2), and (n) PB(1:3). Scan area: 1 μm × 1 μm.

Table 2
Surface roughness parameters of bioplastic films measured by AFM.

Treatment	RMS (nm)	Ra (nm)	Rmax (nm)
Bread Starch	257	184	1525
PVA	11.1	7.17	100
Sago	21.6	17.2	124
PB(1:3)	49	39.9	237
PB(2:2)	78.2	65.1	424
SB(1:3)	104	86	663
SB(2:2)	86.2	68.6	534

approximately 65% at 256 nm, indicating reduced UV-blocking capability compared to bread starch. The PVA film showed the highest UV transmittance at 70% around 241 nm, reflecting its limited ability to block UV radiation due to its synthetic nature and lack of UV-absorbing groups.

All blend films containing bread starch showed minimal UV transmittance, approaching zero at wavelengths below 250 nm. For the composite films, those with higher bread starch content generally displayed lower transmittance, aligning with the trend observed in the Bread starch film. In the visible region (400–800 nm), transparency increased across all films. The PVA film achieved the highest transmittance at over 90%, followed by the Sago film at 85%, indicating excellent clarity. The PB(2:2) and PB(1:3) films followed with 80% and 75% transmittance, respectively. However, PB(1:3) exhibited a greenish hue, which may slightly reduce its perceived transparency despite a relatively high value. The SB(2:2) and SB(1:3) films showed moderate transparency at 70% and 65%, respectively, with the lower values likely due to light scattering by sago starch granules [12]. The Bread starch film had the lowest visible transmittance at 60%, due to light scattering by impurities and its less transparent structure.

These findings confirm that films with higher bread starch content, such as Bread starch and SB(1:3), exhibit UV-blocking properties, while sago starch and PVA-based films (Sago, PVA, PB(2:2)) offer greater transparency in the visible range. The SB formulations balance UV protection and moderate visibility, making them promising for sustainable packaging applications requiring both attributes [33].

3.6. Color characteristics

The color characteristics of the bioplastic films were evaluated using the CIE L*a*b* color space to assess their aesthetic properties for packaging applications. The L* (lightness), a* (red-green axis), b* (yellow-blue axis), and total color difference (ΔE) values were measured, and the results are summarized in Table 3.

The Bread starch film exhibited the lowest lightness (**L*** = 87.04 ± 0.03), suggesting a relatively darker appearance compared to the composite films. This aligns with the inherent opacity of starch-based matrices [35]. Incorporation of sago starch and polyvinyl alcohol (PVA) into the composites significantly enhanced lightness ($p < 0.05$), with the 100% PVA film achieving the highest value (L* = 91.42 ± 0.11), attributed to PVA's high transparency and reduced light scattering [33].

Among the blend films, PB(2:2) and SB(2:2) showed the greatest lightness, likely due to a higher amount of PVA and sago starch contributing to the film clarity. This finding is consistent with Priyadarsini et al. [36] and Taharuddin et al. [37], who demonstrated that the incorporation of PVA and sago starch in guar gum and agar composites, respectively, improved optical transparency by minimizing light diffusion [36,37].

The a* parameter, which indicates redness (positive values) or greenness (negative values), also varied significantly ($p < 0.05$). SB(1:3) and SB(2:2) exhibited the highest redness, possibly due to residual pigments in sago and bread starch. Lau et al. [14] linked such tones to natural starch components. However, Che Hamzah et al. [38] reported increased redness in sago starch films when combined with red cabbage anthocyanin, suggesting that the elevated a* values in SB films may stem from intrinsic sago pigments rather than external colorants [38]. In contrast, PB(1:3) and PB(2:2) blends showed reduced redness and a slight green shift, consistent with PVA's neutral optical properties [33].

The b* values, which reflect yellowness (positive) or blueness (negative), were highest for the Bread starch, followed by SB(1:3) and PB(1:3), with significant differences ($p < 0.05$). The lowest yellowness

Table 3
Color characteristics of bread starch, sago starch, and PVA films and their blends.

Treatments	L*	a*	b*	ΔE
Bread Starch	86.44 ± 0.03^{e}	0.64 ± 0.03^{c}	11.68 ± 0.06^{a}	0.06 ± 0.02^{a}
SB(1:3)	87.19 ± 0.16^{f}	0.99 ± 0.05^{a}	10.25 ± 0.15^{b}	1.49 ± 0.16^{b}
SB(2:2)	88.67 ± 0.06^{d}	0.89 ± 0.01^{b}	8.12 ± 0.03^{d}	3.92 ± 0.04^{d}
Sago	90.41 ± 0.07^{b}	0.28 ± 0.01^{e}	7.80 ± 0.02^{e}	5.15 ± 0.06^{f}
PB(1:3)	88.12 ± 0.07^{d}	0.53 ± 0.01^{d}	9.63 ± 0.21^{c}	2.32 ± 0.20^{c}
PB(2:2)	89.10 ± 0.20^{c}	0.51 ± 0.01^{d}	7.68 ± 0.18^{e}	4.50 ± 0.24^{e}
PVA	91.42 ± 0.11^{a}	0.23 ± 0.01^{f}	6.78 ± 0.04^{g}	6.59 ± 0.09^{g}

Means with different superscript letters within the same column are significantly different ($p < 0.05$) according to Tukey's post-hoc test. Values are presented as Mean ± SD. L* represents lightness, a* represents the red-green axis, b* represents the yellow-blue axis, and ΔE is the total color difference relative to the Bread starch treatment, calculated using the CIELAB formula.

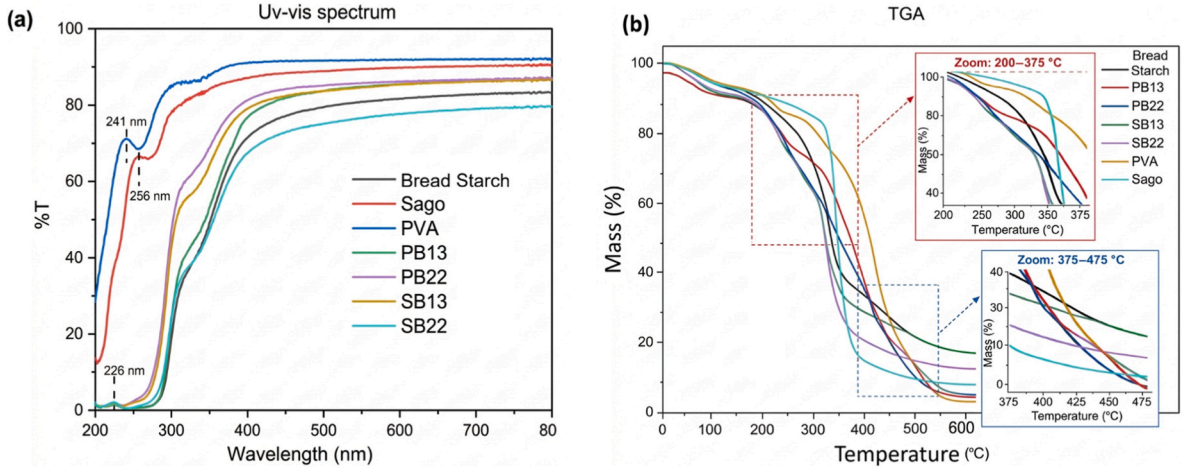

Fig. 5. (a) UV-Vis transmittance spectra of bioplastic films with different treatments in the wavelength range of 200–800 nm. **(b)** TGA curves of bioplastic films with different treatments over a temperature range of 0–600 °C.

was observed in PVA, PB(2:2), and SB(2:2), indicating a shift toward a more neutral hue. This reduction in yellowness with increased PVA or sago content aligns with findings by Mustafa et al. [12], who attributed decreased b* values to enhanced polymer network uniformity [12]. Tambe et al. [39] further corroborated this trend, noting that *Aloe vera* gel in starch–PVA blends reduced yellowness, underscoring the role of PVA in mitigating the yellow tint inherent to starch [39].

The total color difference (ΔE) calculated relative to the Bread starch sample. Moderate deviations were observed in SB(1:3) and PB(1:3), while more pronounced differences were recorded for SB(2:2) and PB (2:2), indicating enhanced color modification due to the higher substitution of bread starch in place of sago starch and PVA. The PVA film exhibited the highest ΔE valuE, reflecting a significant color change from the Bread starch 's darker and yellower profile. This trend underscores the dominant influence of PVA on film color uniformity. Singh et al. [23] similarly reported PVA's stabilizing effect on film optics, while Che Hamzah et al. [38] found that increased additive levels in sago-based films reduced color variability supporting the observed improvements in SB(2:2) and PB(2:2) [38].

From an aesthetic standpoint, the elevated lightness and reduced yellowness of PB(2:2) and SB(2:2) enhance their visual appeal, making them suitable for transparent packaging applications such as fresh produce [40]. In contrast, the Bread starch's darker and yellower appearance may be more appropriate for niche applications where a natural tone is preferred.

3.7. Thermogravimetric analysis (TGA)

Thermal stability is an important property for packaging materials, as it ensures that the material can withstand elevated temperatures during processing, storage, or transportation without degrading [40,41]. TGA was conducted to evaluate the thermal stability and decomposition behavior of the bioplastic films over a temperature range of 0–600 °C. The TGA curves, showing mass loss as a function of temperature, are presented in Fig. 5. All films exhibited three distinct decomposition stages, typical of starch-based bioplastics. The first stage, occurring between 50 °C and 150 °C, corresponds to the evaporation of moisture and volatile components, such as absorbed water and glycerol, resulting in a mass loss of approximately 5–10% across all samples [12]. Composite films showed a slightly higher initial mass loss, likely due to moisture retained in the voids created by interactions between starch and PVA within the polymer matrix. The PVA film exhibited the lowest mass loss in this stage (around 5%), consistent with its synthetic nature and lower moisture content, as noted in the study of PVA/microcrystalline cellulose (MCC) composites, where a similar initial mass loss was observed due to moisture evaporation [42].

The second decomposition stage, occurring between 200 °C and 350 °C, is attributed to the thermal degradation of starch and glycerol, involving the breakdown of glycosidic bonds and the volatilization of plasticizers. The sago film and its blends with bread starch showed a significant mass loss in this stage, dropping to approximately 20% and 30% of their initial mass by 350 °C, respectively, indicating lower thermal stability due to weaker starch-starch interactions than starch-PVA [10]. The PVA film and its blends with bread starch exhibited a slower mass loss rate, retaining 45–60% of their mass at 350 °C. This improved stability is likely due to stronger inter- and intramolecular bonding in PVA, as well as its hydrogen bonding interactions with bread starch, which delay thermal decomposition [43]. Naduparambath et al. [42] reported a similar trend in PVA-MCC composites, where the second stage decomposition occurred between 250 °C and 344 °C, with improved decomposition temperatures due to hydrogen bonding between PVA and MCC [42].

The third decomposition stage, occurring between 350 °C and 500 °C, corresponds to the degradation of the polymer backbone, including the carbonization of starch and the breakdown of PVA chains. The bread starch and sago films continued to lose mass rapidly, reaching around 20% and 10% of their initial mass by 500 °C, respectively. The PVA film showed a more gradual mass loss, retaining approximately 5% of its mass at 500 °C, reflecting its slower but complete degradation lower [44]. The composite films demonstrated intermediate behavior, with SB retaining 15–20% of their mass, while PB retained 10–15%. The higher residual mass in SB films indicates that sago starch contributes to thermal stability at higher temperatures, possibly by forming a more stable char structure, similar to a study on increased thermal stability in sago starch films with anthocyanin at the final degradation stage [38]. This enhancement might be attributed to the higher amylopectin content in sago starch, which forms a more stable matrix with bread starch and glycerol, delaying decomposition [29]. Maryam et al. (2023) reported that adding sago starch nanoparticles to PVA improved bioplastic properties, including thermal stability, due to enhanced intermolecular interactions, supporting the trends observed in SB films [45].

Beyond 500 °C, all films were nearly completely decomposed, leaving 5–20% residual mass.

In general, the incorporation of sago starch increased thermal stability compared to the Bread starch and PB films, particularly in the second and third decomposition stages. This enhancement might be attributed to the higher amylopectin content in sago starch, which forms a more stable matrix with bread starch and glycerol, delaying decomposition [29]. Maryam et al. (2023) reported that adding sago starch nanoparticles to PVA improved bioplastic properties, including thermal stability, due to enhanced intermolecular interactions, supporting the trends observed in SB films [45].

3.8. Water vapor transmission rate (WVTR)

For food packaging, a low WVTR is essential to protect moisture-sensitive products, such as dry goods or snacks, from humidity-induced degradation. The WVTR of the bioplastic films was measured to evaluate their barrier properties, and the results are summarized in Table 3. The bread starch film exhibited a WVTR of 777.43 ± 8.87 g/(m^2·24 h), serving as the baseline for comparison. Sago-starch achieved 649.65 ± 6.63 g/(m^2·24 h), while PVA recorded 571.39 ± 17.69 g/(m^2·24 h), the latter being the most impermeable ($p < 0.05$). The lower WVTR of PVA underscores its superior barrier properties, likely due to its uniform, denser structure compared to starch-based matrices [43]. Incorporation of sago starch in SB films significantly increased WVTR ($p < 0.05$), with SB(1:3) at 786.83 ± 4.43 g/(m^2·24 h) and SB(2:2) at 807.52 ± 9.28 g/(m^2·24 h). This elevation, particularly with the higher sago content, reflects increased permeability, likely due to the lower density of the SB composite and a porous structure in the matrix, as well as the hygroscopic properties of sago starch [14,29]

In contrast, PB films displayed significantly lower WVTR values ($p < 0.05$), indicating enhanced barrier properties with increasing PVA content. Although the difference between PB(1:3) and PB(2:2) was not statistically significant ($p > 0.05$), the trend suggests PVA's role in forming a denser matrix through hydrogen bonding with starch, reducing water vapor pathways. Hendrawati et al. [46] reported that a 30% PVA addition in sago starch foams reduced water absorption to 29.42%, reinforcing the starch barrier-enhancing effect [46]. Tambe et al. [39] further noted a 21.44% WVP reduction in starch–PVA blends with *Aloe vera* gel, attributed to a compact, crosslinked structure, aligning with the improved barrier performance of PB films [39]. The results showed that PB films are optimal for applications requiring robust water vapor barriers, while SB films suit scenarios necessitating moderate permeability.

3.9. Surface hydrophobicity

The contact angle (CA) was measured to evaluate the apparent surface hydrophobicity of bioplastic films. It should be noted that CA is influenced not only by the chemical composition of the surface but also by surface roughness and heterogeneity; therefore, the results should be

interpreted together with the AFM observations The mean CA was calculated as the average of the left and right contact angles from three replicates per treatment (Table 4). Representative CA images for each treatment are shown in Fig. 6, arranged from the most hydrophilic (sago) to the most hydrophobic (PVA), illustrating the droplet behavior on the film surfaces. Plain sago starch exhibited the lowest CA (23.08 ± 4.65°, $p < 0.05$), indicating the highest apparent surface hydrophilicity among all treatments, which aligns with its high amylopectin content that enhances water affinity [29]. This is consistent with findings by Kasim et al. (2023), who reported that sago starch-based edible coatings exhibit low CA values (18.08° to 88.29°), indicating better wettability and hydrophilicity, ideal for coating applications like banana where strong adhesion is needed [47]. However, the CA of starch-based films may also be affected by surface roughness, which can either enhance or reduce the apparent wettability depending on the surface morphology.

PVA exhibited the highest CA (80.56 ± 3.76°), confirming its superior hydrophobic properties compared to starch-based films. However, Jamali et al. [48] observed that pure PVA films have a low CA (27.89°) which might be due to lower glycerol content (1–5 wt%). It was reported that increasing the glycerol content led to an increase in surface hydrophilicity [48], showing that formulation differences can strongly influence the measured CA. The SB films, containing sago starch, also showed relatively low CA values, following the expected trend of increasing hydrophilicity with higher sago starch content. This indicates that the more starch-rich SB formulations remain more wettable, although their apparent CA may also be influenced by their surface topography. This supports the hydrophilic behavior of SB films, where the addition of sago starch enhances polar interactions with water, making SB(2:2) more hydrophilic than SB(1:3), and both more hydrophilic than the bread starch.

In contrast, the PB films, incorporating PVA, demonstrated significantly higher CA values ($p < 0.05$), indicating greater hydrophobicity. PB(1:3) and PB(2:2) had CA values of 67.14 ± 1.46° and 71.49 ± 0.25°, respectively, reflecting the role of PVA in reducing water sensitivity by forming a denser matrix through hydrogen bonding with starch [33]. Chen et al. [31] found that starch films with PVA (degree of polymerization 2400) achieved a CA of 79.81 ± 1.74°, highlighting that PVA can enhance apparent hydrophobicity through intermolecular interactions and film structure. At the same time, surface roughness may also contribute to these differences by modifying droplet spreading and contact-line behavior [31]. The high variability in SB(2:2) (SD = 12.29°) suggests surface heterogeneity, as also indicated by AFM, possibly due to uneven mixing of sago starch with bread starch. Such heterogeneity can affect droplet spreading and make CA values less uniform. Overall, the relatively high CA values of PB(1:3), PB(2:2), and PVA, together with their surface characteristics, suggest suitability for packaging moisture-sensitive products such as dry snacks, where reduced water interaction is beneficial [40]. Conversely, the hydrophilic nature of sago, SB(2:2), and SB(1:3) (CA < 52°) may be advantageous for packaging fresh produce, where some breathability is needed to prevent condensation and microbial growth [49].

Table 4
Contact Angle (CA) and Water Vapor Transmission Rate (WVTR) of bioplastic films with different treatments.

Treatments	CA mean	WVTR (g/(m^2·24h))
Bread starch	57.57 ± 0.8^{bc}	777.43 ± 8.87^{c}
Sago	23.08 ± 4.65^{a}	649.65 ± 6.63^{e}
SB(1:3)	52.00 ± 1.50^{b}	786.83 ± 4.43^{b}
SB(2:2)	48.67 ± 12.29^{b}	807.52 ± 9.28^{a}
PB(1:3)	67.14 ± 1.46^{c}	673.98 ± 4.43^{d}
PB(2:2)	71.49 ± 0.25^{c}	670.84 ± 17.73^{d}
PVA	80.56 ± 3.76^{c}	571.39 ± 17.69^{f}

Different superscripts indicate significant differences ($p < 0.05$) based on one-way ANOVA followed by Tukey's post-hoc test.

3.10. Mechanical properties

The mechanical properties of bioplastic films (thickness: 20 μm), including tensile strength (TS) and elongation at break (EAB), were analyzed to evaluate their potential for food packaging applications. TS measures the maximum stress a film can withstand before breaking, while EAB reflects the film's ability to undergo deformation before rupture. The results are presented in Fig. 7a–c. The Bread starch film had a TS of 2.14 ± 0.20 MPa and an EAB of 84.02 ± 16.51%, reflecting low mechanical strength and limited ability to undergo deformation before failure. This may be due to impurities that interfere with the integrity of the film network, as indicated by SEM and AFM analysis. Plain PVA exhibited the highest tensile strength (16.38 ± 2.08 MPa) and elongation at break (560.03 ± 50.60%), both significantly greater than the other treatments ($p < 0.05$). Its superior mechanical performance is attributed to its strong and highly deformable polymer network. SEM and AFM analyses confirmed a smooth, uniform surface with low roughness (RMS 11.1 nm), supporting efficient stress distribution and high elongation. The sago film exhibited a tensile strength (TS) of 2.08 ± 0.37 MPa, which was not significantly different from that of the Bread starch ($p > 0.05$). However, its elongation at break (EAB) was significantly higher (146.95 ± 50.81%) than the Bread starch ($p < 0.05$), likely due to its high amylopectin content, which facilitates greater network extension under tensile stress. The high variability in Sago's EAB suggests structural inconsistency, possibly due to the presence of fragments shown in SEM, which can disrupt uniformity under tensile stress [35]. The SB films exhibited tensile strength values comparable to the Bread starch and Sago films. Similarly, their elongation at break (≈125%) showed no significant difference from the reference films ($p > 0.05$) indicating similar deformation behaviour prior to failure. These results indicate that incorporating sago starch into bread starch does not significantly enhance mechanical strength. The PB films exhibited improved mechanical properties with increasing PVA content. PB(1:3) showed a tensile strength (TS) similar to starch-based films (2.15 ± 0.32 MPa, $p > 0.05$) but a significantly higher elongation at break (EAB) (~260%, $p < 0.05$), indicating that even 30% PVA enhances the film's ability to deform before breaking despite limited reinforcement. In contrast, PB(2:2) demonstrated markedly higher TS (15.5 ± 0.5 MPa) and similarly high EAB (~260%), both significantly greater than starch-based films ($p < 0.05$), due to the higher PVA content (50%), which promotes stronger hydrogen bonding and intermolecular entanglements. Visual evidence of these mechanical properties is provided in Fig. 6, which shows the stretching behavior of the films during tensile testing. The PVA film exhibits the most significant elongation, consistent with its high EAB, while the Bread starch shows minimal stretching, aligning with its low EAB. Similarly, PB(2:2) demonstrates considerable stretching, reflecting its high TS and EAB, whereas Sago and SB films show moderate elongation, supporting their intermediate deformation capacity. Boonsuk et al. [32] found that PVA in glycerol-plasticized cassava starch blends improves mechanical properties by enhancing film morphology, consistent with the high TS and EAB of PVA and PB (2:2) [32]. Cano et al. [50] reported that PVA incorporation into pea starch films significantly improves flexibility, aligning with the trends observed in PVA and PB(2:2) [50].

Films with high tensile strength and high elongation at break like PVA and PB(2:2) are well suited for packaging applications that require durability and the ability to withstand deformation without failure, such as for heavier or flexible goods [28]. In contrast, films with lower strength and moderate elongation at break like bread and sago starch and their composite are more appropriate for lightweight packaging applications, such as wrapping fresh produce, where extreme mechanical performance is not required [47].

3.11. Cost benefit analysis

Table 5 compares the PB(2:2) film with conventional bioplastic

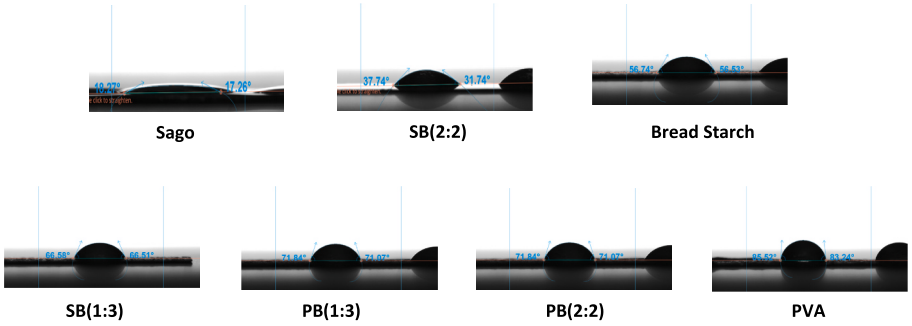

Fig. 6. Representative contact angle images of bioplastic films, ordered by increasing hydrophobicity from sago (Most Hydrophilic) to PVA (Most Hydrophobic).

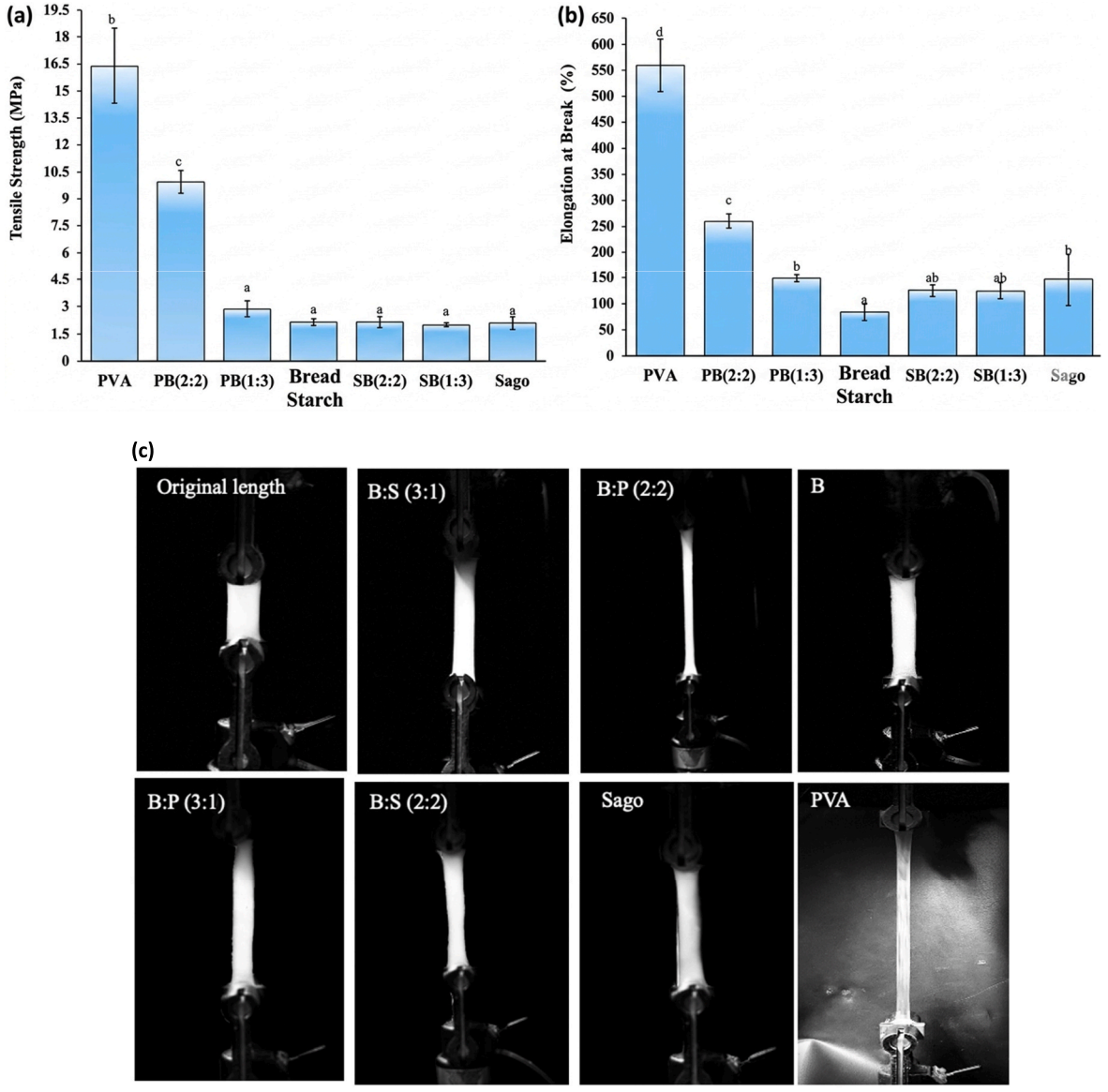

Fig. 7. Mechanical properties of bioplastic films across different treatments. (a) Tensile Strength (TS, MPa) and (b) Elongation at Break (EAB, %) of bioplastic films. (c). Representative images from tensile testing illustrating the deformation and fracture behavior of the films.

polymers such as pure PVA, PLA, and PHA in terms of mechanical, barrier, and economic performance. We incorporate a conservative valorization cost of $0.20/kg to account for collection, drying, and processing. According to the PB(2:2) film composition, we also includes glycerol at $1.30/kg, which is a common plasticizer in starch–PVA blends. The total estimated production cost of the PB(2:2) film is approximately $1.87/kg, significantly lower than pure PVA ($4.0/kg), PLA ($2.5–3.0/kg), and PHA (~$5.0–7.0/kg).

In addition to its economic advantage, the PB(2:2) film demonstrated a tensile strength of 19.95 MPa and elongation at break of 259.99%,

Table 5
Cost-benefit analysis comparing the PB(2:2) bioplastic film with pure PVA, PLA, and PHA in terms of material cost, mechanical performance, environmental impact, and suitability for packaging applications. Bread starch is considered a zero-cost feedstock, highlighting the economic and ecological advantages of food waste valorization.

Parameter	PB(2:2) Film (Bread Starch + PVA)	Pure PVA Film ([51]; e.V., 2023)	PLA (Polylactic Acid) [51,52]	PHA (Polyhydroxyalkanoates) [53–56]
Raw Material Cost	**Low (bread starch = $0/kg)** + PVA (~$4/kg) + Glycerol ($1.3/kg)	(~$4/kg)	(~$2.5–3.0/kg)	(~$5–7/kg)
Bread Waste Valorization	$0.20/kg (**Valorization**: collection, treatment, drying and storage)	None	None	None
Tensile Strength (MPa)	19.95 MPa (PB2:2)	~30 MPa	~50–70 MPa (brittle)	~20–40 MPa
Elongation at Break (%)	259.99%	560%	5–10% (very brittle)	10–30%
UV-blocking Ability	Excellent (0% @ 294 nm)	Poor	Moderate	Moderate
Water Vapor Barrier (WVTR)	657.67 g/m^2/day	600–650 g/m^2/day	~350–500 g/m^2/day	~200–400 g/m^2/day
Biodegradability	High	Moderate	High	Very High
Surface Appearance	Smooth, transparent	Transparent	Often hazy	Slightly opaque
Economic Circularity	**Strong**: upcycles food waste	None	None	None
Estimated Production Cost ($/kg)	**~$1.87** (including $0.20/kg valorization cost in lab scale)	~$4.0	~$2.5–3.0	~$5.0–7.0

"PLA: commercial-grade polylactic acid typically used for food packaging. PHA: medium-chain-length polyhydroxyalkanoates from microbial fermentation as reported in relevant literature. Properties vary with grade, processing, and source."

indicating good mechanical flexibility suitable for packaging. While its strength is lower than pure PVA and PLA, the film offers excellent UV-blocking ability (0% transmittance at 294 nm) and a competitive water vapor barrier (WVTR = 657.67 g/m^2·day). Its smooth, transparent surface and high biodegradability further position it as a strong alternative for applications demanding sustainable, low-cost materials. The PB(2:2) system also upcycles food waste into value-added products, reinforcing its alignment with circular economy goals. While PLA and PHA films are known for their biodegradability and moderate to high barrier properties, their significantly higher raw material costs ($2.5–7.0/kg) and brittleness (especially in PLA) may limit flexibility in end-use applications. In contrast, the PB(2:2) film combines low cost, good transparency, and functionality, although further optimization may be required to enhance its mechanical durability for broader commercial use.

The production cost of the bioplastic films was estimated based on the raw material composition of each formulation using a mass-balance approach.

The unit prices used in the calculation were based on conservative market values and literature reports. Bread waste was assumed to have negligible cost because food waste is typically available at zero or negative value due to disposal costs, as widely reported in food waste management studies ([57,58]). The cost of starch extraction from bread waste was estimated at $0.2/kg in lab scale. This value represents the operational cost associated with low-intensity wet extraction involving drying, milling, water extraction, sedimentation, and drying, without the use of chemical reagents. Similar food-waste starch recovery processes have been reported to fall within the range of $0.1–0.4/kg, supporting the conservative estimate used in this study [8,59].

The material cost per kilogram of film was calculated by multiplying the weight fraction of each component by its corresponding unit price and summing the individual contributions according to the following equation:

$$Film\ cost(\$/kg) = \sum (w_i \times C_i) \quad \text{Eq. (3)}$$

Since all formulations were prepared using the same casting procedure under identical laboratory conditions, processing-related costs such as energy, labor, and equipment were assumed to be comparable and were therefore excluded to enable a fair comparison of formulation-dependent material costs. This approach is commonly adopted in preliminary economic assessments to evaluate the relative feasibility of alternative material compositions.

Bread waste was assumed to have negligible raw material cost because food waste is generally available at minimal or negative value due to disposal expenses ([57,58]). The cost of starch recovered from bread waste was estimated at approximately $0.2/kg, representing the operational cost of a low-intensity wet extraction process involving drying, milling, water extraction, sedimentation, and drying without chemical reagents. Similar food-waste starch recovery processes have been reported within the range of $0.1–0.4/kg [8,60]. The market prices of PVA and glycerol were assumed to be $4.0/kg and $1.3/kg, respectively, based on industrial bulk price ranges reported in recent market analyses and literature sources [61].

Based on these values, the PB(2:2) formulation exhibited a production cost of approximately $1.87/kg. The results in Table 4 indicate that incorporating bread waste–derived starch significantly reduces the overall material cost while maintaining desirable functional properties. Considering that the market price of conventional bioplastic packaging materials such as PLA and other new emergent commercial biopolymer films typically ranges between $2 and $7/kg [62], the proposed formulation demonstrates promising economic potential for sustainable packaging applications.

4. Conclusions

This study successfully developed bioplastic films from bread waste, sago starch, PVA, and glycerol, demonstrating their potential for food packaging through comprehensive analyses. Molecular and structural analyses confirmed effective blending with physical interactions enhancing compatibility, while morphological studies revealed smoother surfaces in PVA and PB films, correlating with superior mechanical strength. Optical tests showed a balance between UV-blocking and transparency, thermal analysis indicated improved stability in SB films, and barrier properties varied, with PB films excelling for moisture-sensitive products and SB films suiting breathable packaging. Hydrophobicity was higher in PVA and PB films, while mechanical tests highlighted their exceptional strength and flexibility compared to starch-based films.

A key outcome is the effective use of bread waste, preserving its functionality in the films while maintaining high mechanical and other properties. The optimal formulation, particularly PB(2:2), utilizes bread waste to balance performance and cost-effectiveness, offering a sustainable alternative to conventional plastics. This approach reduces production costs while meeting the demand for eco-friendly packaging, with PB(2:2) excelling in clarity, UV-blocking, thermal stability, barrier properties, hydrophobicity, and mechanical strength. SB films, with moderate permeability and hydrophilicity, are ideal for fresh produce packaging, enhancing the versatility of these bread waste-based

materials in sustainable applications. Overall, the PB(2:2) formulation presents a promising, cost-effective, and high-performance bioplastic, demonstrating that upcycling food waste can simultaneously enhance material properties and reduce production costs, advancing both environmental and economic goals in sustainable packaging. This study provides a practical roadmap for industries to incorporate food, agricultural waste, and biomass into bioplastic formulations, enabling cost reduction while maintaining or enhancing material functionality.

Based on the obtained data, the PB (2:2) bioplastic film is well-suited for packaging applications such as fresh produce, owing to its excellent UV-blocking ability, high transparency, good mechanical strength, and moderate moisture barrier. Additionally, for respiring products like berries, mushrooms, and leafy greens, the inherent gas permeability of starch/PVA-based films may offer a preferable alternative to conventional plastic films that require puncturing. This allows for controlled gas exchange without compromising the film's integrity, making PB (2:2) a promising sustainable solution for medium shelf-life fresh food packaging.

CRediT authorship contribution statement

Shima Jafarzadeh: Writing – original draft, Validation, Project administration, Methodology, Investigation, Formal analysis. **Peng Wu:** Writing – original draft, Methodology, Data curation, Conceptualization. **Moon Paul:** Methodology, Formal analysis. **Zeinab Qazanfarzadeh:** Writing – original draft, Data curation. **Colin J. Barrow:** Writing – review & editing, Validation, Supervision. **Omid Zabihi:** Writing – original draft, Methodology. **Wendy Timms:** Writing – review & editing, Supervision, Resources. **Minoo Naebe:** Writing – review & editing, Validation, Supervision.

Declaration of competing interest

The authors declare that they have no known competing financial interests or personal relationships that could have appeared to influence the work reported in this paper.

Acknowledgments

The authors acknowledge funding from School of Engineering and the Centre for Sustainable and Bioproducts at Deakin University.

Data availability

Data will be made available on request.

References

[1] S. Jafarzadeh, Z. Qazanfarzadeh, N. Oladzadabbasabadi, M. Naebe, C.J. Barrow, Transforming nutshell waste into next-generation bioplastics for a sustainable and circular economy, Biomass Bioenergy 210 (2026) 109061.
[2] S. Jafarzadeh, Z. Yildiz, P. Yildiz, P. Strachowski, M. Forough, Y. Esmaeili, M. Naebe, M. Abdollahi, Advanced technologies in biodegradable packaging using intelligent sensing to fight food waste, Int. J. Biol. Macromol. 261 (2024) 129647.
[3] F. Berry, M. Retamal, U. Kuzhiumparambil, P. Ralph, Market and Sustainability Potential for Algal Bioplastics in Australia, 2022.
[4] S. Jafarzadeh, M. Golgoli, M. Azizi-Lalabadi, J. Farahbakhsh, M. Forough, N. Rabiee, M. Zargar, Enhanced carbohydrate-based plastic performance by incorporating cerium-based metal-organic framework for food packaging application, Int. J. Biol. Macromol. 265 (2024) 130899.
[5] S. Jafarzadeh, Z. Qazanfarzadeh, E. Parandi, Y. Esmaeili, C.J. Barrow, W. Timms, M. Naebe, Eco-friendly plastics from cereal-derived by-products and waste: a circular economy approach for sustainable packaging, Mater. Today Chem. 47 (2025) 102782.
[6] S. Talekar, K. Ekanayake, B. Holland, C. Barrow, Food waste biorefinery towards circular economy in Australia, Bioresour. Technol. 388 (2023) 129761.
[7] H. Churton, B.K. McCabe, Advancing a food loss and waste bioproduct industry: a critical review of policy approaches for application in an Australian context, Heliyon 10 (12) (2024) e32735.
[8] V. Narisetty, R. Cox, N. Willoughby, E. Aktas, B. Tiwari, A.S. Matharu, K. Salonitis, V. Kumar, Recycling bread waste into chemical building blocks using a circular biorefining approach [10.1039/D1SE00575H], Sustain. Energy Fuels 5 (19) (2021) 4842–4849, https://doi.org/10.1039/D1SE00575H.
[9] P. Gupta, B. Toksha, M. Rahaman, A review on biodegradable packaging films from vegetative and food waste, Chem. Rec. 22 (7) (2022) e202100326.
[10] B. Wang, B. Yu, C. Yuan, L. Guo, P. Liu, W. Gao, D. Li, B. Cui, A. Abd El-Aty, An overview on plasticized biodegradable corn starch-based films: the physicochemical properties and gelatinization process, Crit. Rev. Food Sci. Nutr. 62 (10) (2022) 2569–2579.
[11] S. Jafarzadeh, A. Alias, F. Ariffin, S. Mahmud, A. Najafi, S. Sheibani, Characterization of a new biodegradable edible film based on semolina loaded with nano kaolin, Int. Food Res. J. 24 (1) (2017).
[12] P. Mustafa, M.B.K. Niazi, Z. Jahan, S. Rafiq, T. Ahmad, U. Sikander, F. Javaid, Improving functional properties of PVA/starch-based films as active and intelligent food packaging by incorporating propolis and anthocyanin, Polym. Polym. Compos. 29 (9) (2021) 1472–1484.
[13] C.-y. Su, D. Li, L.-j. Wang, Y. Wang, Biodegradation behavior and digestive properties of starch-based film for food packaging–a review, Crit. Rev. Food Sci. Nutr. 63 (24) (2023) 6923–6945.
[14] W.N. Lau, A.M. Nafchi, M. Zargar, N.H.M. Rozalli, A.M. Easa, Development and evaluation of Bauhinia Kockiana extract-incorporated sago starch intelligent film strips for real-time freshness monitoring of coconut milk, Int. J. Biol. Macromol. 260 (2024) 129589.
[15] S. Azmin, I. Nasrudin, M. Mat Nor, P. Abdullah, H. Ch'Ng, Development of food packaging bioplastic from potato peel starch incorporated with rice husk silica using response surface methodology comprehending central composite design, Food Res. (2024).
[16] L. Behera, M. Mohanta, A. Thirugnanam, Intensification of yam-starch based biodegradable bioplastic film with bentonite for food packaging application, Environ. Technol. Innov. 25 (2022) 102180.
[17] S. Das, M.I. Kalyani, From trash to treasure: review on upcycling of fruit and vegetable wastes into starch based bioplastics, Prep. Biochem. Biotechnol. 53 (7) (2023) 713–727.
[18] L. Hamid, S. Elhady, A. Abdelkareem, I. Fahim, Fabricating starch-based bioplastic reinforced with bagasse for food packaging, Circ. Econ. Sustain. 2 (3) (2022) 1065–1076.
[19] S. Jafarzadeh, M. Paul, N. Oladzad-abbasabadi, P. Wu, C.J. Barrow, M. Naebe, W. Timms, Bioactive bioplastic films incorporating waste-derived carbon dots and starch for sustainable packaging, Matter (2026).
[20] S. Paidari, Y. Esmaeili, S.A. Ibrahim, S. Vahedi, S.A. Al-Hilifi, N. Zamindar, Application of nanoparticles to enhance the microbial quality and shelf life of food products, in: Microbial Biotechnology in the Food Industry: Advances, Challenges, and Potential Solutions, Springer, 2024, pp. 75–102.
[21] A. Setiawan, R.N. Mahfud, N.E. Mayangsari, D.R. Widiana, A.P. Iswara, D. Dermawan, The potential of using sweet corn (Zea mays Saccharata) husk waste as a source for biodegradable plastics, Ind. Crop. Prod. 208 (2024) 117760.
[22] Z. Qazanfarzadeh, H. Baptista, C. Nunes, V. Kumaravel, Development of smart food packaging from bread waste-derived starch and carbon quantum dots, Ind. Crop. Prod. 233 (2025) 121426.
[23] S. Singh, S. Gaur, N. Sharma, Starchy films as a sustainable alternative in food industry: current research and applications, Starch Staerke 76 (11–12) (2024) 2300078.
[24] R. Dewi, N. Sylvia, M. Riza, Characterization of degradable plastics from Sago and breadfruit starch-based with addition of zinc oxide (ZnO) catalyst and polyvinyl alcohol (PVA), Jurnal Kimia Sains dan Aplikasi 26 (11) (2023) 427–436.
[25] M.G. Kupervaser, M.V. Traffano-Schiffo, M.L. Dellamea, S.K. Flores, C.A. Sosa, Trends in starch-based edible films and coatings enriched with tropical fruits extracts: a review, Food Hydrocolloids for Health 4 (2023) 100138.
[26] N. Tabassum, U. Rafique, M. Qayyum, A.A. Mohammed, S. Asif, A. Bokhari, Kaolin–polyvinyl alcohol–potato starch composite films for environmentally friendly packaging: optimization and characterization, J. Compos. Sci. 8 (1) (2024) 29.
[27] T. Soliman, S. Vshivkov, Effect of Fe nanoparticles on the structure and optical properties of polyvinyl alcohol nanocomposite films, J. Non-Cryst. Solids 519 (2019) 119452.
[28] J. Zanela, M. Casagrande, M.O. Reis, M.V.E. Grossmann, F. Yamashita, Biodegradable sheets of starch/polyvinyl alcohol (PVA): effects of PVA molecular weight and hydrolysis degree, Waste Biomass Valoriz. 10 (2019) 319–326.
[29] G.O. Al-Fakih, R. Ilyas, M. Huzaifah, A. El-Shafay, Recent advances in sago (Metroxylon sagu) fibres, biopolymers, biocomposites, and their prospective applications in industry: a comprehensive review, Int. J. Biol. Macromol. (2024) 132045.
[30] N.H.C. Hamzah, N. Khairuddin, I.I. Muhamad, S.R. Sarbini, Response surface methodology for controlling the release of anthocyanin from sago starch films, Polym. Bull. (2024) 1–16.
[31] Y. Chen, H. Zhang, G. Wei, F. Liu, Y. Zhang, Y. Chen, Active starch-based film using polyvinyl alcohol and Chlorogenic acid for strawberry preservation: a comparative analysis of mechanical, barrier, and antibacterial properties, Food Chem. (2025) 143027.
[32] P. Boonsuk, A. Sukolrat, K. Kaewtatip, S. Chantarak, A. Kelarakis, C. Chaibundit, Modified cassava starch/poly (vinyl alcohol) blend films plasticized by glycerol: structure and properties, J. Appl. Polym. Sci. 137 (26) (2020) 48848.
[33] J.R.V. Matheus, R.R. Dalsasso, E.A. Rebelatto, K.S. Andrade, L.M.d. Andrade, C.J. d. Andrade, A.R. Monteiro, A.E.C. Fai, Biopolymers as green-based food packaging materials: a focus on modified and unmodified starch-based films, Compr. Rev. Food Sci. Food Saf. 22 (2) (2023) 1148–1183.

[34] M.-C. Popescu, B.-I. Dogaru, M. Goanta, D. Timpu, Structural and morphological evaluation of CNC reinforced PVA/starch biodegradable films, Int. J. Biol. Macromol. 116 (2018) 385–393.
[35] E. Basiak, A. Lenart, F. Debeaufort, How glycerol and water contents affect the structural and functional properties of starch-based edible films, Polymers 10 (4) (2018) 412.
[36] P. Priyadarsini, M. Biswal, S. Gupta, S. Mohanty, S.K. Nayak, Development and characterization of ester modified endospermic guar gum/polyvinyl alcohol (PVA) blown film: approach towards greener packaging, Ind. Crop. Prod. 187 (2022) 115319.
[37] N.H. Taharuddin, R. Jumaidin, R.A. Ilyas, Z.H. Kamaruddin, M.R. Mansor, F.A. Md Yusof, V.F. Knight, M.N.F. Norrrahim, Effect of agar on the mechanical, thermal, and moisture absorption properties of thermoplastic sago starch composites, Materials 15 (24) (2022) 8954.
[38] N.H. Che Hamzah, N. Khairuddin, I.I. Muhamad, M.A. Hassan, Z. Ngaini, S. R. Sarbini, Characterisation and colour response of smart sago starch-based packaging films incorporated with Brassica oleracea anthocyanin, Membranes 12 (10) (2022) 913.
[39] S.S. Tambe, S. Zinjarde, A.A. Athawale, Aloe vera gel–reinforced biodegradable starch–PVA blends for sustainable packaging of green chillies, Packag. Technol. Sci. 37 (7) (2024) 605–617.
[40] G. Khaleel, V.S. Sharanagat, S. Upadhyay, S. Desai, K. Kumar, A. Dhiman, R. Suhag, Sustainable approach toward biodegradable packaging through naturally derived biopolymers: an overview, Journal of Packaging Technology and Research (2024) 1–28.
[41] N. Oladzadabbasabadi, M.A. Dheyab, M. Tavassoli, M. Naebe, S. Jafarzadeh, M. Ghasemlou, E.P. Ivanova, B. Adhikari, Leveraging lignin as mussel-bioinspired adhesives and fillers for sustainable food-packaging applications: a review, Int. J. Biol. Macromol. 318 (2025) 145029.
[42] S. Naduparambath, M. Sreejith, T. Jinitha, V. Shaniba, K. Aparna, E. Purushothaman, Development of green composites of poly (vinyl alcohol) reinforced with microcrystalline cellulose derived from sago seed shells, Polym. Compos. 39 (9) (2018) 3033–3039.
[43] Z. Zamrud, W. Ng, H. Salleh, Effect of bentonite nanoclay filler on the properties of bioplastic based on sago starch, IOP Conf. Ser. Earth Environ. Sci. (2021).
[44] B. Fauzi, M.G.M. Nawawi, R. Fauzi, N.I.M. Ismail, D.A.B. Sidik, N.S.M. Aripen, F.A. M. Rosdan, D.K. Sohami, Enhancing biodegradability and functionality of packaging films: a statistical approach of Sago Starch nanocomposite, Future Energy and Environment Letters 1 (1) (2024) 48–59.
[45] A.K. Maryam, E. Novelina, Improvement on the bioplastic properties of polyvinyl alcohol (PVA) with the sago starch nanoparticle addition, Sylwan 166 (1) (2022).
[46] N. Hendrawati, K. Sa'diyah, E. Novika, A.A. Wibowo, The effect of polyvinyl alcohol (PVOH) addition on biodegradable foam production from sago starch, in: AIP Conference Proceedings, 2020.
[47] R. Kasim, N. Bintoro, S. Rahayoe, Y. Pranoto, Physiological activity of banana coated with sago starch and cellulose nanofiber edible coating, IOP Conf. Ser. Earth Environ. Sci. (2021).
[48] A.R. Jamali, A.A. Shaikh, A.D. Chandio, Preparation and characterisation of polyvinyl alcohol/glycerol blend thin films for sustainable flexibility, Mater. Res. Express 11 (4) (2024) 045102.
[49] K. Makhijani, R. Kumar, S.K. Sharma, Biodegradability of blended polymers: a comparison of various properties, Crit. Rev. Environ. Sci. Technol. 45 (16) (2015) 1801–1825.
[50] A.I. Cano, M. Cháfer, A. Chiralt, C. González-Martínez, Physical and microstructural properties of biodegradable films based on pea starch and PVA, J. Food Eng. 167 (2015) 59–64.
[51] C. Kourmentza, J. Plácido, N. Venetsaneas, A. Burniol-Figols, C. Varrone, H. N. Gavala, M.A. Reis, Recent advances and challenges towards sustainable polyhydroxyalkanoate (PHA) production, Bioengineering 4 (2) (2017) 55.
[52] B. Laycock, P. Halley, S. Pratt, A. Werker, P. Lant, The chemomechanical properties of microbial polyhydroxyalkanoates, Prog. Polym. Sci. 38 (3–4) (2013) 536–583.
[53] D.B.M. Research, Global polyhydroxyalkanoates (PHA) market size, share, and trends analysis report – industry overview and forecast to 2032. https://www.databridgemarketresearch.com/reports/global-polyhydroxyalkanoate-pha-market, 2024.
[54] K. Sudesh, H. Abe, Y. Doi, Synthesis, structure and properties of polyhydroxyalkanoates: biological polyesters, Prog. Polym. Sci. 25 (10) (2000) 1503–1555.
[55] R. Auras, B. Harte, S. Selke, An overview of polylactides as packaging materials, Macromol. Biosci. 4 (9) (2004) 835–864.
[56] G.-Q. Chen, M.K. Patel, Plastics derived from biological sources: present and future: a technical and environmental review, Chem. Rev. 112 (4) (2012) 2082–2099.
[57] J. Parfitt, M. Barthel, S. Macnaughton, Food waste within food supply chains: quantification and potential for change to 2050, Phil. Trans. Biol. Sci. 365 (1554) (2010) 3065–3081, https://doi.org/10.1098/rstb.2010.0126.
[58] The state of food and agriculture: moving forward on food *loss and waste reduction*. https://openknowledge.fao.org/server/api/core/bitstreams/11f9288f-dc78-4171-8d02-92235b8d7dc7/content.
[59] M. Bjerg-Nielsen, A.J. Ward, H.B. Møller, L.D.M. Ottosen, Influence on anaerobic digestion by intermediate thermal hydrolysis of waste activated sludge and co-digested wheat straw, Waste Manag. 72 (2018) 186–192, https://doi.org/10.1016/j.wasman.2017.11.021.
[60] L. Dai, H. Yu, J. Zhang, F. Cheng, Preparation and characterization of cross-linked starch nanocrystals and self-reinforced starch-based nanocomposite films, Int. J. Biol. Macromol. 181 (2021) 868–876, https://doi.org/10.1016/j.ijbiomac.2021.04.020.
[61] polyvinyl alcohol (PVOH) market. https://www.marketsandmarkets.com/Market-Reports/polyvinyl-alcohol-pvoh-market-106878201.html.
[62] BIOPLASTICS MARKET DEVELOPMENT UPDATE. https://www.european-bioplastics.org/market/, 2025.